Published online 19 June 2012 Nucleic Acids Research, 2012, Vol. 40, No. 16 7739–7752
doi:10.1093/nar/gks545

Regulation of p21/CIP1/WAF-1 mediated cell-cycle arrest by RNase L and tristetraprolin, and involvement of AU-rich elements

Latifa Al-Haj[1], Perry J. Blackshear[2] and Khalid S.A. Khabar[1,*]

[1]Program in BioMolecular Research, King Faisal Specialist Hospital and Research Centre, Riyadh 11211, Saudi Arabia and [2]National Institute of Health, Research Triangle Park, NC 27709, USA

Received January 14, 2012; Revised and Accepted May 9, 2012

ABSTRACT

The p21$^{Cip1/WAF1}$ plays an important role in cell-cycle arrest. Here, we find that RNase L regulates p21-mediated G_1 growth arrest in AU-rich elements-dependent manner. We found a significant loss of p21 mRNA expression in *RNASEL*$^{-/-}$ MEFs and that the overexpression of RNase L in HeLa cells induces p21 mRNA expression. The p21 mRNA half-life significantly changes as a result of RNase L modulation, indicating a post-transcriptional effect. Indeed, we found that RNase L promotes tristetraprolin (TTP/*ZFP36*) mRNA decay. This activity was not seen with dimerization- and nuclease-deficient RNase L mutants. Deficiency in TTP led to increases in p21 mRNA and protein. With induced ablation of RNase L, TTP mRNA and protein expressions were higher, while p21 expression became reduced. We further establish that TTP, but not C124R TTP mutant, binds to, and accelerates the decay of p21 mRNA. The p21 mRNA half-life was prolonged in *TTP*$^{-/-}$ MEFs. The TTP regulation of p21 mRNA decay required functional AU-rich elements. Thus, we demonstrate a novel mechanism of regulating G_1 growth arrest by an RNase L-TTP-p21 axis.

INTRODUCTION

Ribonuclease L (RNase L) is an interferon (IFN) inducible endoribonuclease and constitutes a first line of defense against viruses, which is further activated during IFN response (1–2). RNase L is further activated by 2′–5′-oligoadenylates, which are synthesized from ATP by oligoadenylate synthase (OAS). The expression of OAS is induced by IFN, and its activity is trigged by double-stranded viral RNA (3). RNase L has other functions, including pro-apoptotic effects (1,4), anti-proliferative action (5–6), muscle differentiation regulation (7) and senescence induction (8). Unlike its antiviral action, the molecular mechanisms underlying RNAse L action on cellular growth and the cell cycle are poorly understood.

The cell cycle is a tightly regulated and orchestrated process. It progresses from one phase to another and is controlled by a group of cyclins, cyclin-dependent kinases (Cdk) and other factors. The Cdk activity is regulated by a group of inhibitors (CKI) that regulate the cell cycle's progression. Among these is p21$^{Waf1/Cip1}$ (Also, called CDKN1A; hereafter referred to as p21), which has a wide spectrum of inhibitory effects on G_1 CDK–cyclin complexes (9). This cellular growth arrest at the G_1 phase occurs in a variety of human and animal somatic cells in response to external stimuli. The p21 protein level is induced in response to DNA damage, which participates in growth arrest [Reviewed in: (10,11)]. This occurs by p21 binding to and inhibiting the activity of cyclin–Cdk2/Cdk4, resulting in the inhibition of cell-cycle progression from G_1 to the S phase (9) or, in other words, G_1 arrest. The p21 gene (CDKN1A) is a direct target for the tumor suppressor protein p53, which is an essential mediator of p21-regulated growth suppression and cellular senescence (12).

The post-transcriptional regulation of p21 gene expression by the RNA-binding protein HuR has been shown (13,14). HuR is one of many RNA-binding proteins that recognizes AU-rich elements (ARE), which exist in >15% of the human and mouse transcriptomes (15). AREs are among the most characterized mRNA decay-promoting and translation-inhibitory sequences and can be recognized by an array of RNA-binding proteins. Aberrations of ARE-mediated pathways can be associated with certain chronic inflammatory conditions and cancer, as was recently reviewed by us in (16). Among the RNA-binding proteins that are known to interact with ARE sequences are the zinc-finger protein 36 (ZFP36), C3H type, homolog (mouse), also known as tristetraprolin (TTP), ZFP36L1 (zinc-finger protein 36, C3H type-like 1, also known as BRF1); and TIA1

*To whom correspondence should be addressed. Tel: +966 1 442 7876; Fax: +966 1 442 4182; Email: khabar@kfshrc.edu.sa

(TIA1 cytotoxic granule-associated RNA-binding protein) (17).

In this report, we find that RNase L binds and regulates TTP expression. As a result, we also show that TTP directly binds to and promotes the decay of the p21 mRNA in an ARE-dependent manner. The induced ablation of RNase L diminishes the p21-mediated growth arrest, indicating that constitutive RNase L is essential for the p21 pathway. These events establish a novel mechanism whereby RNase L causes p21-mediated growth arrest by a process that is dependent on TTP's activity on p21 ARE.

MATERIALS AND METHODS

Cell culture

WISH (HeLa markers) and human embryonic kidney HEK293 cell lines were obtained from the American Type Culture Collection (ATCC; Rockville, MD) and maintained in Dulbecco's modified Eagle's medium (DMEM) (Invitrogen, Carlsbad, CA) supplemented with 10% fetal bovine serum (FBS) and antibiotics. The hepatocarcinoma cell line Huh-7 was obtained from Dr Stephen Polyak (University of Washington, Seattle, WA) and was cultivated in DMED (Invitrogen, Carlsbad, CA) supplemented with 10% FBS and antibiotics. Mouse embryonic fibroblast (MEF) lines (*RNase* $L^{+/+}$ and *RNase* $L^{-/-}$) were generated from C57BL/6 mice as previously described (1). The $TTP^{+/+}$ and $TTP^{-/-}$ mouse embryonic fibroblasts were generated from TTP (ZFP36)-knockout mice as previously described (18) and were grown in DMEM (Invitrogen, Carlsbad, CA) supplemented with 10% FBS and antibiotics. The irradiator, an X-RAD 320 Precision X-ray INC, (North Branford, CT) was used to transfer 10 Gy (Co-60 gamma-rays, 97–112 cGy/min) or sham irradiation (0 Gy) immediately to the culture medium.

Plasmids and cloning of ARE reporter plasmids

Wild-type TTP and mutant C124R were sub-cloned into pCR3.1 as previously described (19). RNase L–HA and Exon3 deleted-HA coding regions were synthesized by (GENEART) and subcloned in pcDNA 3.1. The Exon3 deleted coding region is a frame shift at codon 493 with additional 18 amino acids and premature stop codon at 513 and thus is it considered a C-terminal deletion variant. The R462Q RNase L is provided by Dr Robert H. Silverman (Cleveland Clinic, OH) and was fused with HA tag at C-terminus by PCR and subcloned in pcDNA3.1. The RNase L C-terminal deletion mutant was provided also by Dr Robert H. Silverman.

PCR3.1-C124R construct fused with wild-type TTP 3′-UTR was constructed by inserting the TTP 3′-UTR region (1040–1745) onto pCR3.1-C124R plasmid using EcoR V and XbaI restriction enzymes to replace BGH 3′-UTR. TTP 3′-UTR was amplified using oligonucleotides that included EcoR V (GATATC) and Xba I (TCT AGA) restriction sites. Sense oligonucleotide sequence is 5′-GCAGCGATATCCAAAGTGACTGCCCGGTC-3′-and antisense; 5′-GCAGCTCTAGAACACTCAGAT TGTTTATTTA-3′. Linear PCR product was digested with EcoR V and Xba I and purified and subsequently ligated to linear PCR3.1-C124R plasmid.

The region that contains putative AU-rich element sequences, which correspond to the ARE-containing stretches in the 3′-UTRs of p21/CDKN1A (NM_000389; 685–749 nt for ARE-containing sequence) was used to design synthetic complementary oligonucleotides of 70 bases, with BamHI and XbaI overhangs. The p21/CDKN1A oligonucleotide ARE sequence is:

TAGTCTCAGTTTGTGTGTCTTAATTATTATTTG TGTTTTAATTTAAACACCTCCT. The p21 mutant ARE (with three single base mutations bolded and underlined) TAGTCTCAGT**C**TGTGTGTCTTAATT ATTATTTGTGT**C**TTAAT**C**TAAACACCTCCTC.

Short DNA duplexes were made by annealing the two synthetic complementary oligonucleotides of 70 bases. The oligonucleotides were designed to contain (G/**GATC C**) BamHI and (**T**/CTAGA) XbaI underlined overhangs. The short DNA duplexes were subsequently ligated into EGFP plasmid (Gene Therapy Systems, Inc., San Diego, CA), which was modified to contain a RPS30M1/Intron constitutive promoter (20). After ligation and transformation, recombinant colonies were verified by PCR, using a forward vector specific primer and an ARE reverse primer.

Transfection and reporter activity assessment

HEK293 cells seeded into a 96-well clear-bottom black microplate were cotransfected with 100 ng of the ARE-containing reporters and 100 ng of either PCR3.1, wild-type TTP, or mutant C124R, using lipofectamine 2000 reagent (Invitrogen). Transfections were performed in several replicates. The variance in GFP fluorescence among replicate microwells was <6%; thus, with this minimum variance, experiments do not warrant transfection normalization (21). Automated laser-focus image capture was performed using the high-throughput BD Pathway 435 imager (BD Biosciences, San Jose, CA). Image processing, segmentation and fluorescence quantification was facilitated by the ProXcell program as previously described (22). Data are presented as mean values ± standard error (SEM) of total fluorescence intensity in each well, with replicate readings ranging from three to four as indicated in the text. A Student *t*-test was used when comparing the two data groups.

Real-time PCR

Quantitative real-time PCR for human and mouse TTP and RNase L was performed using a custom-made Taqman primer and probe set (Applied Biosystems). The endogenous control human and murine GAPDH or ACTB mRNA probe labeled with a 5′-reporter VIC dye (Applied Biosystems) were used for normalization. For SybrGreen Real-Time PCR, total RNAs were treated with DNase I and cDNAs were used with Lightcycler faststart DNA master SYBR Green I, (Roche, USA). The primers for the SybrGreen real-time PCRs were as follow: murine p21/CDKN1A sense (CGAGAACGGTG

GAACTTTGAC); antisense (CAGGGCTCAGGTAGA CCTTG); human p21/CDKN1A; sense (TGGAGACTC TCAGGGTCGAAA); antisense (GGCGTTTGGAGTG GTAGAAATC); human GAPDH sense (GGCAAATT CAACGGCACAGT); antisense (AGATGGTGATGGG CTTCCC); murine GAPDH sense (GCCTGCTTCACCA CCTTCT); antisense (CCCCAATGTGTCCGTCGTG). Specific oligonucleotide primers were used to detect transfected TTP. The sequence is; sense, 5′-CATCTTCAATCG CATCTCTGT-3′-targeting TTP coding region, and antisense, 5′-TAGAAGGCACAGTCGAGG-3′-targeting BGH 3′-UTR. For transfected C124R fused with TTP 3′-UTR, we used the following primers: Oligonucleotide sequences is; sense, 5′-CATCTTCAATCGCATCTCTGT-3′, targeting TTP coding region and antisense, 5′-TTAAG CGTAATCCGGAACATCGTAT-3′-targeting HA tag at C124R C-terminus. In all cases, relative quantification of gene expression was determined using the standard curve method and the values obtained were within both detectable and linear range. Average concentrations were normalized to the endogenous GAPDH or ACTB gene. The final results were converted to Ratios ± SEM of the specific mRNA levels to housekeeping mRNA levels. Real time PCR was performed in multiplex in the Chroma 4 DNA Engine cycler (Bio-Rad).

Western blotting

Total lysates were prepared in RIPA buffer (10 mM Tris–HCl, 15 mM NaCl, 1.5 MgCl2, 1% Triton X-100, 0.25% sodium deoxycholate, 1 mM PMSF, 1× proteinase inhibitors cocktail). Immunoblotting was developed and bands were quantified using ImageJ 1.44 software (NIH, USA) and normalized to ACTB. The following commercial antibodies were used for immunoblotting: anti-TTP (N-18), anti-p21 (F-5), from Santa Cruz Biotech, Santa Cruz, CA. Other antibodies used in this study include anti-RNASE L (Novus Biologics), anti-β-actin (Abcam, MA) and anti-HA (Roche Biosciences).

RNA EMSA, supershift and *in vitro* TTP translation

An RNA gel-shift assay was carried out as previously described (23), with minor modifications. Briefly, total lysate from HEK293 overexpressing either wild-type TTP or mutant C124R was incubated with custom-synthesized (Metabion) 5′-end-biotin-labeled sense RNA oligonucleotides corresponding to p21 ARE and mutant ARE (Figure 6C). The assay was carried out as described previously (23). For supershift, anti-TTP antibody (Santa Cruz) was pre-incubated with the lysate for 30 min before the addition of the labeled probe.

Immunoprecipitation of RNP complexes

For RNase L-HA IP, HECK293 cells were seeded into 100 × 20 mm culture dishes, and the next day, they were transfected with either pcDNA3.1, RNase L-HA, R462-HA, or Exon3 deleted-HA constructs. After 24 h, immunoprecipitations were arried out as previously described (19,24). Briefly, lysates from different groups were incubated with 100 µl of anti-hemagglutinin (HA) (Roche diagnostics, Germany) or normal IgG (Santa Cruz) coated pre-swollen A/G agarose beads (Santa Cruz Biotech, Santa Cruz, CA). Next, the beads were washed, and genomic DNA and proteins were sequentially removed by digestion with RNAse-free DNAse I and Proteinase K. Purified RNAs were reverse-transcribed into cDNAs and subjected to real-time quantitative PCR (qPCR), using a Human TaqMan expression assay for p21, TTP and GAPDH as a housekeeping control. Real time PCR was run on Chroma 4 thermocycler instrument (Bio-Rad). For TTP IP, HEK293 cells were transfected with either PCR3.1, wild-type TTP, or C124R plasmid. Next, IP was performed using anti-TTP (N-18) (Santa Cruz Biotech, Santa Cruz, CA) or normal IgG (Santa Cruz Biotech, Santa Cruz, CA).

mRNA half-life determinations

For mRNAs half-lives determination, actinomycin D (5 µg/ml) was added to the culture medium, and after the indicated times, the total RNAs were extracted, followed by DNase digestion for eliminating DNA contamination, cDNA syntheses. The cDNAs were used for QPCR. Standard curves for each gene were generated to determine the relative concentrations of amplified transcripts. The concentration of each transcript was then normalized to GAPDH or β-actin mRNA levels, and the normalized values were used to calculate the half-lives. One-phase exponential decay curve analysis (GraphPad Prism) was used to assess mRNA decay kinetics.

For C124R (fused with wild-type TTP 3′-UTR) mRNA half-life determination, Huh7 cells seeded into six-well plate were transfected with construct containing C124R fused with TTP 3′-UTR along with pcDNA3.1 vector control or RNase L. Similarly, actinomycin D half-life experiment was carried out as described above and cDNAs were subjected to real-time PCR using SybrGreen method.

Flow cytometry analysis

Confluent cells maintained for a period of three days were synchronized at G_1/S by treating cells with 5 µg/ml aphidicholin (Sigma) for 20 h. Then, cells were washed with phosphate-buffered-saline (PBS) and released into the S phase in complete medium with 15% serum. After the indicated times, cells were trypsinized, washed with PBS, fixed with chilled 70% ethanol and kept at 4°C. Cell suspensions were washed with PBS and then incubated in PBS containing RNase (0.1 mg/ml) and propidium iodide (25 µg/ml) for 30 min at 37°C. Then, they were subjected to cell-cycle determination using flow cytometry.

siRNA and shRNA transfection

The sense and antisense siRNA duplexes were from Metabion. The sequence for TTP sense is: GACGGAAC TCTGTCACAAG; and antisense: CTTGTGACAGAGT TCCGTC. The scrambled siRNA sense sequence is: GCG CGCTTTGTAGGATTCGTT; and antisense: CGAATC CTACAAAGCGCGCTT. An amount of 25 µM of siRNAs were used to transfect Huh7 cells (TTP siRNA),

using lipofectamine 2000 reagent (Invitrogen). The silencing of TTP was assayed 48 h post-transfection using immunoblotting. One microgram of shRNAs (control or RNase L) was used to transfect the HEK293 cells. The RNase L target sequence for the shRNA is (CG AAGATGTTGACCTGGTC). Immunoblotting was used to assay for RNase L silencing after 48 h.

Statistical analysis

All comparisons were performed with the Student's paired *t*-test, aided by GraphPad Prism software (San Diego, CA). Significance was reported with two-tailed $P < 0.005$, unless otherwise described.

RESULTS

RNase L-mediated cell-cycle arrest and p21 expression

To explore the capacity of RNase L to attenuate cell-cycle progression, we utilized a polyclonal WISH cell line (HeLa-derived) that stably expresses a moderate level of RNase L and grows slower than the control cells (5). We performed flow cytometric analyses to monitor the cell-cycle progression of aphidicholin-synchronized cells. Upon release into the serum-containing medium, we observed that in RNase L-overexpressing cells, more cells were in the G_0/G_1 phase, and a reduced number of cells were in the S phase, suggesting G_0/G_1 arrest (Figure 1A). We then performed a similar analysis by utilizing the mouse embryonic fibroblast lines (MEFs)

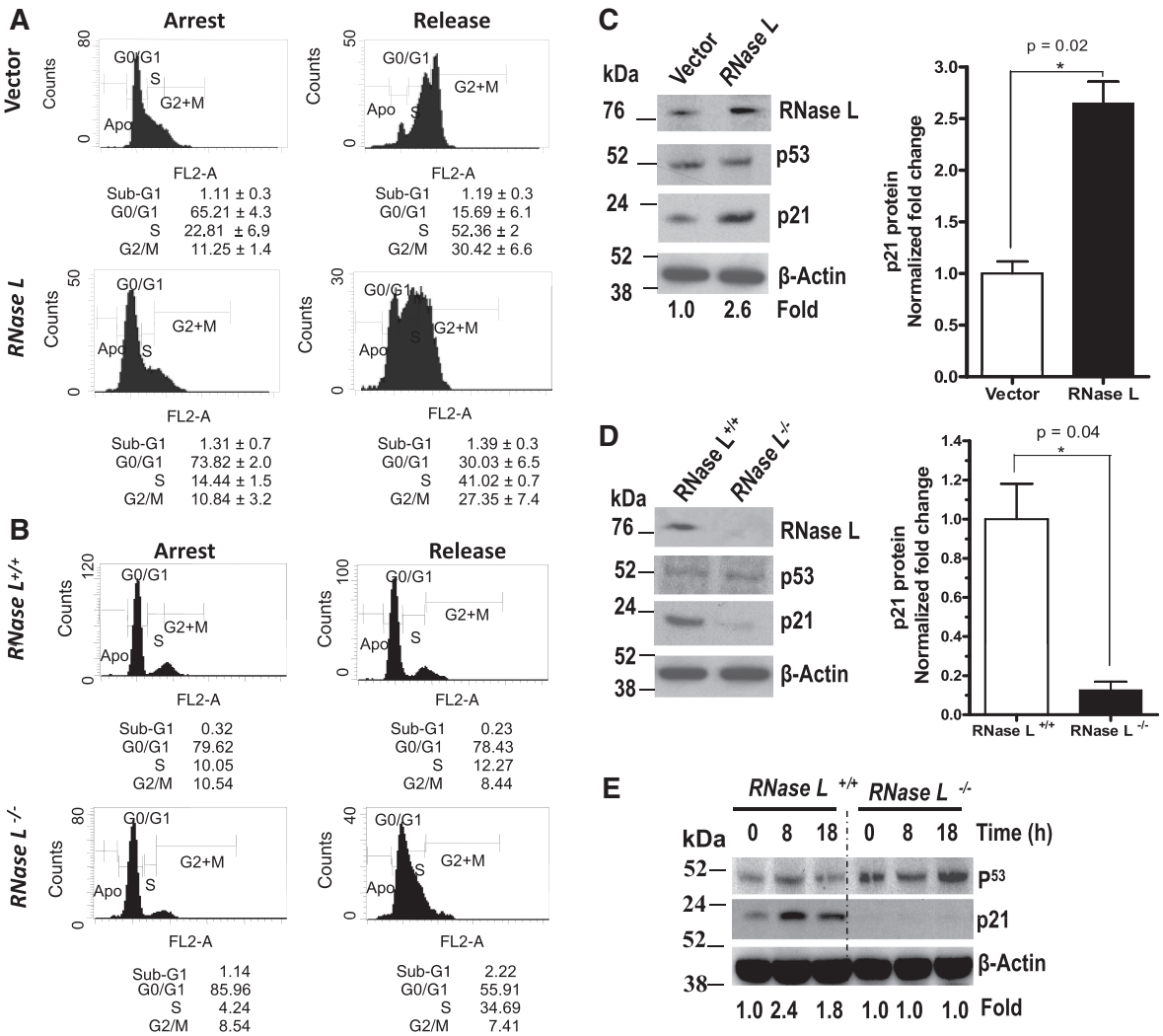

Figure 1. RNase L-mediated cell-cycle arrest and p21 induction. (**A**) Flow cytometric analysis of RNase L polyclonal and control cells. Cells were synchronized at the G_1 phase by confluency and aphidicholin treatment for 18 h. Cells were released by 15% FBS for 6 h and were then subjected for flow cytometry. (**B**) Flow cytometric analysis for cell-cycle profiles of *RNase* $L^{+/+}$ and *RNase* $L^{-/-}$ mouse embryonic fibroblasts. (**C**) Expression of p21 and p53 proteins in RNase L-expressing HeLa cells and vector-expressing cells. Cell lysates were subjected to western blotting using specific antibodies. The p21 band intensities were quantified using (ImageJ 1.44 software), and β-actin normalized fold differences were calculated (*right panel*). The results are represented as the mean ± SEM of two independent experiments. (**D**) *RNase* $L^{+/+}$ and *RNase* $L^{-/-}$ MEF cells lysates were subjected to western blotting for p53 and p21 levels, using specific antibodies for p53 and p21. The results of β-actin normalized band intensities are represented as the mean ± SEM of two independent experiments. (**E**) Wild-type and RNase L-deficient cells were treated with 10 Gy of γ-radiation and incubated for the indicated times. Total cell lysates were analyzed for western blotting, using specific antibodies for p21 and p53.

generated from *RNase L*-knockout and control mice (1). At post-arrest release, *RNase L*-null cells accumulated more at the S phase and had lower G_0/G_1 populations when compared to *RNase* $L^{+/+}$-intact cells (Figure 1B). These results indicate that RNase L may mediate the G_1 arrest of the cell cycle.

In order to find the candidate factor(s) that participate in the cell cycle and allow RNase L to exert its cell-cycle arrest activity, we utilized a model of cell-cycle arrest due to DNA damage by γ-radiation. We performed a western blotting screen of proteins and phosphorylated proteins involved in G_1 and G_2 checkpoints (*Data not shown*) and found that p21 is among those that distinctively associate with RNase L. Thus, we focused our attention on p21 as a potential target in the RNase L pathway of cellular growth suppression.

RNase L overexpression caused p21 protein elevation, but did not cause significant changes in p53 protein levels (Figure 1C). Undetectable basal levels of p21 in *RNase L*-null cells were observed (Figure 1D); as a result of γ-irradiation, there was still no induction of p21 in *RNase L*-null cells at both 8 or 18 h post- irradiation, while wild-type cells with intact RNase L responded to radiation and expressed p21 (Figure 1E).

RNase L modulation of p21 mRNA expression

Next, we assessed the effect of RNase L on the mRNA level of p21 using quantitative PCR (qPCR). We detected very low levels of p21 mRNA in *RNase L*- null cells when compared to wild-type cells (Figure 2A) in agreement with the protein level (Figure 1D). To evaluate whether RNase

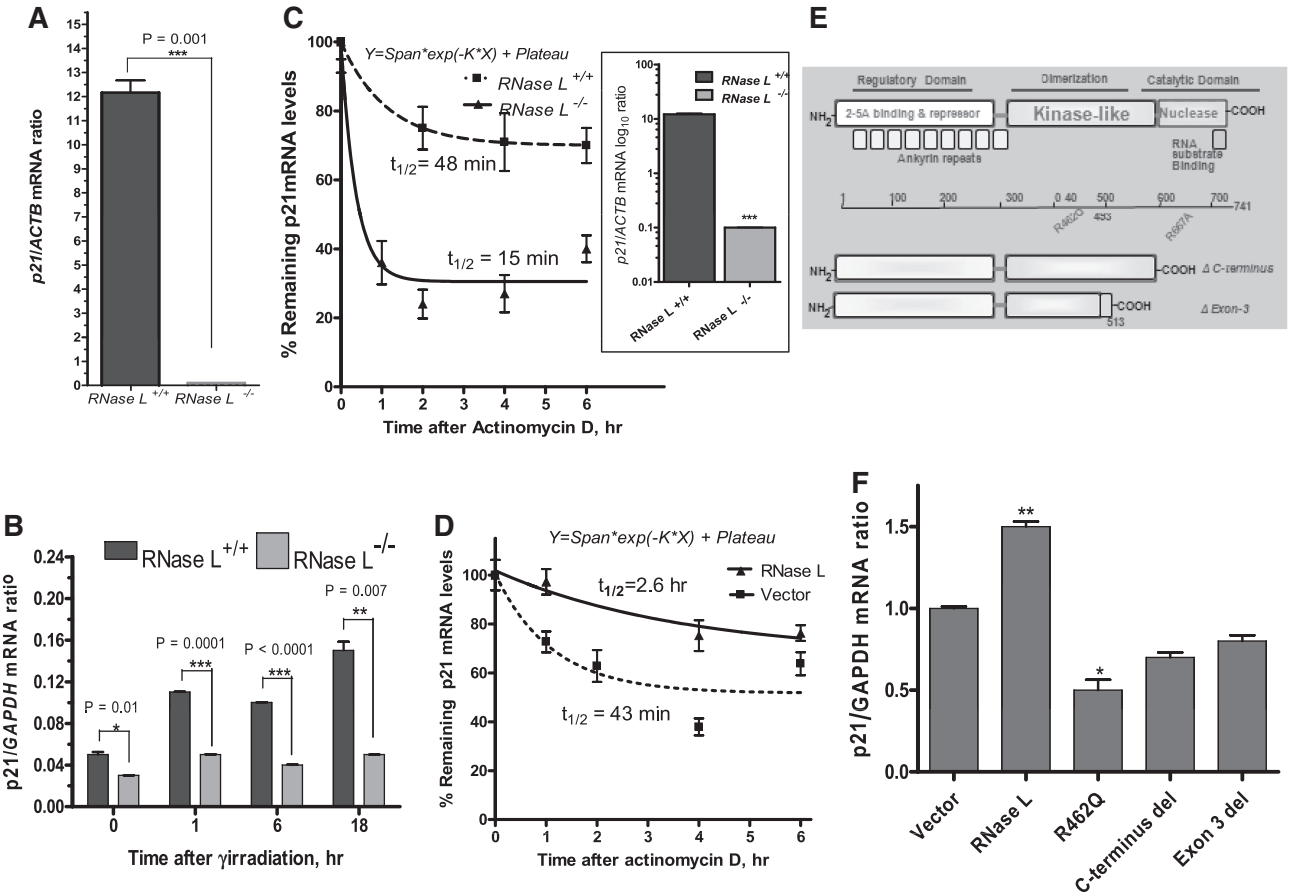

Figure 2. RNase L modulates p21 mRNA expression. (**A**) The p21 mRNA expression in *RNase* $L^{+/+}$ and *RNase* $L^{-/-}$ MEFs. Total RNA was extracted and subjected to RT–qPCR by using specific TaqMan probes for p21. Results are represented as the Mean ± SEM of three independent experiments, each with duplicate readings. (**B**) *RNase* $L^{+/+}$ and *RNase* $L^{-/-}$ MEFs were treated with 10 Gy of γ-radiation and incubated for the indicated times. Total RNAs were extracted and subjected to RT-QPCR for p21 mRNA expression. Data are represented as the mean ± SEM of two independent experiments. *P*-values were calculated using a Student's *t*-test. (**C**) RNase L prolongs the half-life of p21 mRNA. Actinomycin D (AcD) (5 μg/ml) was added to the culture medium of *RNase* $L^{+/+}$ and *RNase* $L^{-/-}$ cells for the indicated times, followed by total RNA extraction and cDNA synthesis. p21 mRNA half-life was calculated using one-phase exponential decay curve analysis (20) (GraphPad Prism) to assess mRNA decay kinetics. Data are from one representative experiment of at least two independent experiments. *Right panel* inset shows the basal levels of p21 mRNA—i.e. before actinomycin D addition, as $\log_{10}$ values. (**D**) The p21 mRNA half-life determination in stable RNase L-overexpressing polyclonal RNase L cells. Data are represented as the mean ± SEM of two independent experiments, using the same protocol as in the C legend. (**E**) Schematic diagram showing the domain structure of wild-type RNase L and mutant variants (*R462Q, Δ-Cterm, or Δ-exon3*). (**F**) The p21 mRNA expression as influenced by wild-type and mutant variants. HEK293 cells overexpressing *RNase L, R462Q, Δ-C terminal mutant, or Δ-exon3 variant* were used to quantify relative p21 mRNA expression. The results are represented as the mean ± SEM of two independent experiments. *P*-value are $*P < 0.01$ and $**P < 0.001$ (Student's *t*-test).

L still regulates p21 mRNA levels during DNA damage, the *RNase L* wild-type and RNase L-null cells were irradiated with γ-radiation (10 Gy) to induce G_1 arrest. In the absence of RNase L, there was a significant reduction of the p21 mRNA level during DNA damage as compared to wild-type cells (Figure 2B). Thus, RNase L modulates p21 mRNA both at the basal and γ-radiation-induced levels.

We assessed the mRNA half-life of p21 in the *RNase L*-knockout MEFs using an actinomycin D chase experiment and the one-phase exponential decay model with β-actin mRNA normalization. The p21 mRNA in the wild-type cells had an apparent half-life of nearly 48 min, but as a result of RNase L ablation in the *RNase* $L^{-/-}$ MEFs, it became highly unstable (apparent half-life of 15 min; Figure 2C). In support of the observed increased decay rate of p21 mRNA in *RNase L* -null cells, the mRNA stability was increased, with an apparent mRNA half-life of 2.6 h in RNase L overexpressing HeLa cells, in contrast to vector control cells, which had an apparent mRNA half-life of 43 min. (Figure 2D). These results suggest that an RNase L-mediated pathway has a role in p21 mRNA stability.

In order to further understand the role of RNase L in p21 mRNA modulation, we evaluated the consequences of overexpressing the wild-type RNase L, the dimerization-deficient R462Q mutant RNase L, the RNase L-deficient exon 3-deleted variant, and the C-terminal domain-deleted mutants. The last two forms lack the nuclease domain (Figure 2E). The expression level of the p21 transcript in HEK293 cells overexpressing the wild-type RNase L was increased (1.5-fold, $P = 0.01$), but not with R462Q or the nuclease-deficient domains (Figure 2F), indicating that both the dimerization domain and the terminal catalytic nuclease domain are required for the RNase L-mediated upregulation of p21 mRNA levels. Apparently, there are dominant negative effects of the mutant forms of RNase L; since these mutants were able to reduce p21 mRNA levels, particularly, the R462Q variant (Figure 2F).

RNase L-mediated stabilization of p21 mRNA is associated with the repression of an mRNA decay protein

The above observations indicate that RNase L leads to p21 mRNA upregulation in a manner that requires the nuclease domain of RNase L, suggesting that RNase L's action upon p21 mRNA regulation is indirect. Indeed, this may be the case. By using RNA-binding protein immunoprecipitation (RNA-IP) followed by quantitative RT–PCR, RNase L was not able to bind to p21 mRNA (Figure 3A). As a control, however, it was able to bind to its putative cellular mRNA target, HuR mRNA, which we previously identified (5) (Figure 3A). Thus, we hypothesized that RNase L mediates its effect through the regulation of an mRNA decay-promoting intermediate. We evaluated the expression of the mRNA-binding proteins TTP, ZFP36L1 and TIA in cells overexpressing wild-type RNase L. We observed a significant reduction (60% reduction, $P < 0.001$) of TTP mRNA in cells overexpressing wild-type RNase L in contrast to the dimerization-deficient *R462Q* (Figure 3B). Western blotting confirmed that the forced overexpression of wild-type RNase L, but not the R462Q or the RNase domain-deleted variant, led to downmodulation of TTP (Figure 3C).

To elaborate on this further, we examined the role of RNase L in controlling TTP in detail. Both the mRNA and protein levels of TTP were elevated in RNAse L-null MEFs when compared to wild-type MEFS (Figure 3D and E, respectively). Further confirmation was obtained using RNA interference experiments; HEK293 cells, which lack or have very low amounts of TTP, were transfected with *RNase L* shRNA or control shRNA. Significant increases in both mRNA (Figure 3F) and protein levels of TTP (Figure 3G) were observed in the RNAse L shRNA-transfected cells. Figure 3G also shows the efficiency of the RNase L knockdown. These data confirm that knockdown of RNase L in human cells functionally parallels the mouse data in Figure 3D.

Binding of RNase L to TTP and mRNA half-life changes

Because RNase L was able to reduce TTP mRNA, we tested RNase L binding to *TTP* mRNA. We overexpressed hemaglutinin (HA) tagged wild-type RNase L (RNase L-HA) or the two mutant forms of RNase L (R462Q-HA and exon3 deleted-HA) in HEK293 cells and then performed RNA-IP, using HA antibody followed by RT–qPCR for *TTP* mRNA. RNase L showed a remarkable ability to bind to TTP mRNA (>50-fold increase, $P < 0.001$) in comparison to R462Q or the RNase-deficient (exon3-deleted) variant (Figure 4A). These results indicate the requirement of the dimerization and the nuclease domain of RNase L for *TTP* mRNA binding. Thus, we identified TTP mRNA as a novel cellular mRNA target for RNase L action.

An actinomycin D chase experiment was performed to determine the decay rate of *TTP* mRNA in *RNase* $L^{-/-}$ and *RNase* $L^{+/+}$ fibroblasts. Unlike the increased basal mRNA levels, the *TTP* mRNA was unstable in *RNase* $L^{-/-}$ cells with an apparent half-life of ~10 min, in contrast to 36 min in *RNase* $L^{+/+}$ fibroblasts (Figure 4B). Further confirmation of this phenomenon was obtained with an RNase L-overexpressing HeLa cell line, in which RNase L caused *TTP* mRNA stabilization (Figure 4C). These results may not be surprising since RNase L is an endoribonuclease that reduces mRNA levels in non-exonuclease manner, while the higher TTP protein levels in RNase $L^{-/-}$ lead to its own (TTP) mRNA half-life reduction (25,26). This is further confirmed by performing a series of experiments in which we employed the zinc-finger mutant TTP C124R that has a point mutation that led to the loss of binding the ARE in the target mRNA (27). First, we show that TTP but not the mutant, C124R, binds to its own (TTP) mRNA (Figure 4D). Then, we nullified the ability of TTP to act on its own mRNA by fusing C124R coding region with its full-length TTP 3′-UTR (Figure 4E, upper panel). The apparent transfected C124R mRNA half life (~3.2 h)

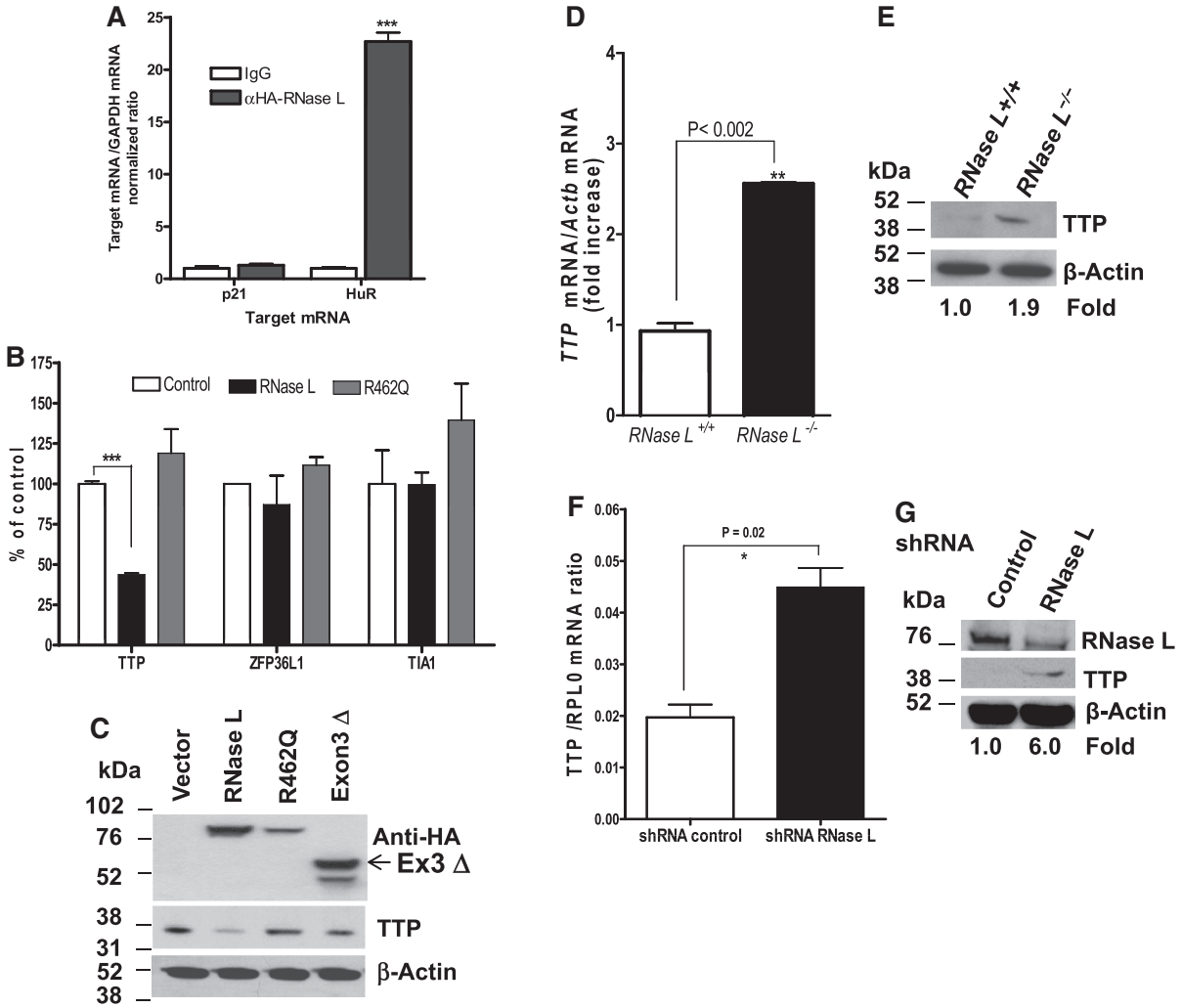

Figure 3. RNase L-mediated stabilization of p21 mRNA is associated with the repression of an RNA decay-promoting protein. (**A**) Real-time PCR determination of endogenous *HuR* and p21 transcripts physically associated with RNase L. Lysate from HEK293 cells transfected with HA tagged RNase L or control vector were used in immunoprecipitation. Immunoprecipitation was carried out using anti-HA or IgG antibody. The results are represented as the mean ± SEM of two independent experiments. $***P < 0.0001$ (Student's *t*-test). (**B**) Real-time PCR monitoring of endogenous TTP, ZFP36L1 and TIA1 transcripts associated with the overexpression of wild-type *RNase L* or mutant variant *R462Q*. The results are represented as the mean ± SEM of two independent experiments, $***P < 0.001$ (Student's *t* test). (**C**) Immunoblotting for HA tagged wild-type and mutants RNase L using anti-HA antibody, and TTP (using anti-TTP antibody) in Huh-7 cells overexpressing wild-type *RNase L*, *R462Q mutant, or Δ-exon3 form (a truncated protein of ~54 kDa due to exon 3 deletion-induced premature termination-See Figure 2E*). All of these constructs are tagged by HA for detecting the expressed proteins from the transfected constructs. β-Actin was used as a loading control. (**D**) Real-time PCR monitoring of endogenous *TTP* transcript. Fold change was normalized to the mouse β-Actin housekeeping gene. The results are represented as the mean ± SEM of two independent experiments. $**P < 0.001$ (Student's *t*-test). (**E**) Immunoblotting of TTP in *RNase* $L^{+/+}$ and *RNase* $L^{-/-}$ mouse embryonic fibroblasts. Band intensities were quantified using ImageJ 1.44 software, and fold differences were calculated. (**F**) QPCR for endogenous TTP transcript associated with RNase L silencing. Fold increase was normalized to human large ribosomal protein (RPL0) housekeeping gene. The results are represented in terms of the mean ± SEM of two independent experiments. $*P = 0.02$ (Student's *t*-test). (**G**) The immunoblotting of endogenous TTP associated with silencing of RNase L. Huh-7 cells were transfected with shRNA for RNase L or control shRNA, and western blotting was performed for RNase L, TTP, or β-actin.

was longer than wild-type TTP (46 min) indicating that loss of its auto-degradation (Figure 4C and E, Vector control curves). In such case, RNase L destabilizes the C124R mRNA (half life is now 39 min, a change from 3.2 h) due to also lack of C124R action on its 3′-UTR (Figure 4E). Using a different strategy for further confirmation, we fuse TTP coding region with a stable bovine growth hormone (BGH) 3′-UTR that lacks ARE and TTP binding (Figure 4F, upper panel). TTP without its 3′-UTR was very stable (>6 h), but was significantly destabilized when RNase L was overexpressed (Figure 4F). The data demonstrate that reduction of TTP mRNA is by RNase L endoribonucleoytic activity (Figure 3B and Figure 4A) even if RNase L tends to stabilize TTP mRNA due to the auto-degradation of TTP mRNA by its own protein.

TTP regulates p21 mRNA stability

Once it was established that RNase L regulates TTP, we asked whether RNase L action on p21 is mediated

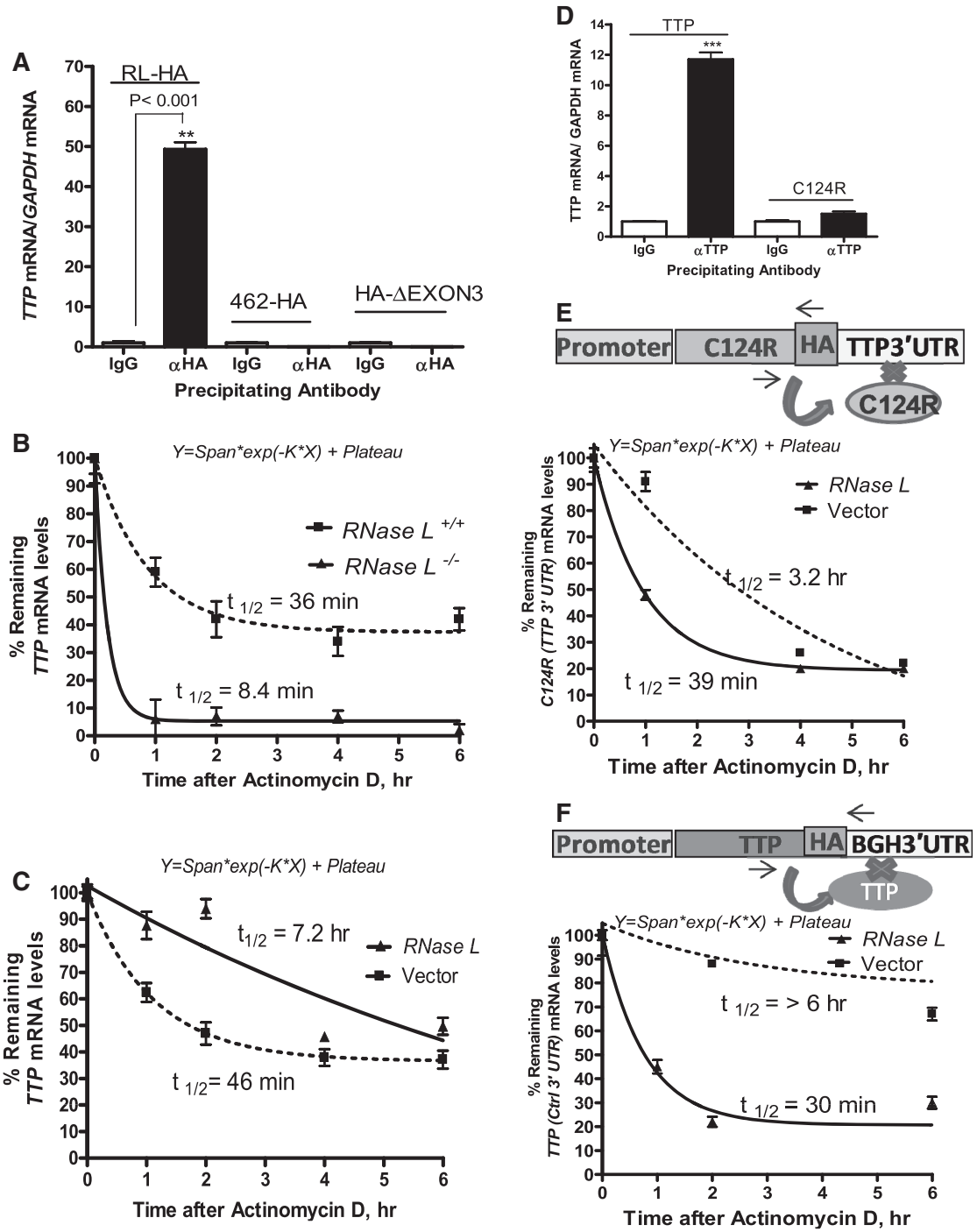

Figure 4. RNase L regulates TTP mRNA stability. (**A**) Real-time QPCR of endogenous *TTP* mRNA physically associated with RNase L or mutant variants (R462Q or Δ exon3) and precipitated with anti-HA antibody (IP-RNA protocols are detailed in 'Materials and Methods' section). The results are represented as the mean ± SEM of two independent experiments. $^{**}P < 0.001$ (Student's *t*-test). (**B**) *TTP* mRNA half-life determination in *RNase* $L^{+/+}$ and *RNase* $L^{-/-}$ mouse embryonic fibroblasts. (**C**) TTP mRNA half-life determination in RNase L-overexpressing HeLa cell line. (**D**) Real-time QPCR of *TTP* mRNA extracted from RNA material physically associated with wild-type TTP or C124R and obtained by precipitation with either anti-TTP antibody or control IgG (IP-RNA protocols are detailed in 'Materials and Methods' section). (**E**) Half-life determination of mRNA generated from the transfected C124R plasmid bearing TTP 3′ UTR in Huh7 cells overexpressing pcDNA3.1 vector or RNase L. (**F**) Half-life determination of mRNA generated from transfected TTP plasmid bearing control stable BGH 3′ UTR in Huh7 cells overexpressing pcDNA3.1 vector or RNase L. In all mRNA half-life determination above, actinomycin D (AcD; 5 μg/ml) was added to the culture medium for the indicated times, followed by total RNA extraction and cDNAs synthesis. To amplify only transfected but not endogenous TTP, specifically positioned primers were used (arrows indicate PCR primers). The TTP mRNA half-life was calculated using one-phase exponential decay curve analysis (GraphPad Prism).

indirectly through the repression of TTP expression. To investigate this, we first needed to prove that the p21 expression is regulated by TTP. We assessed both the mRNA and the protein levels of p21 in *TTP*-deficient ($TTP^{-/-}$) and wild-type *MEFs*. Indeed, the p21 mRNA and protein levels were elevated by 2- and 6-fold, respectively, in *TTP*-null cells in comparison with wild-type cells (Figure 5A and B). Actinomycin D chase experiments demonstrated that p21 mRNA stability was enhanced in $TTP^{-/-}$ MEFs, with an apparent half-life of 2.2 h as compared to 1.4 h in the control cells (Figure 5C).

To assess the potential interaction of TTP with the p21 mRNA, we overexpressed wild-type TTP in HEK293 cells and then performed RNA-IP using a TTP specific antibody. We then performed RT–qPCR on a TTP-bound mRNA population using a primer specific to p21 mRNA. Indeed, TTP showed a strong binding ability towards *p21* mRNA with a >9-fold increase when compared to GAPDH housekeeping mRNA (Figure 5D, left columns). Also, HEK293 cells were transfected with C124R; as a result, the complete loss of binding to p21 mRNA was observed (Figure 5D, right columns). Thus, we identified p21 as a novel mRNA target for TTP action.

TTP regulation of p21 mRNA is AU-rich element dependent

Since AREs are involved in TTP-mediated mRNA decay, we evaluated the involvement of p21 ARE elements in the TTP-mediated decay of p21 mRNA. We utilized EGFP reporter fused with RPS30 cellular promoter to minimize transcriptional promoter induction by modulating the expression vectors (20). Briefly, we fused the reporter coding region with a 70-nt region that spans the putative ARE of p21 mRNA or with a control 70-nt of human growth hormone GH1 (non-ARE sequence) (Figure 6A). The EGFP-fused constructs were cotransfected into HEK293 cells with either wild-type TTP or the zinc-finger mutant TTP (C124R). Ectopic expression of TTP strongly destabilized the p21 ARE-containing 3′-UTR, with a 70% reduction in the GPF level when compared to vector control (Figure 6B). In contrast, the expression

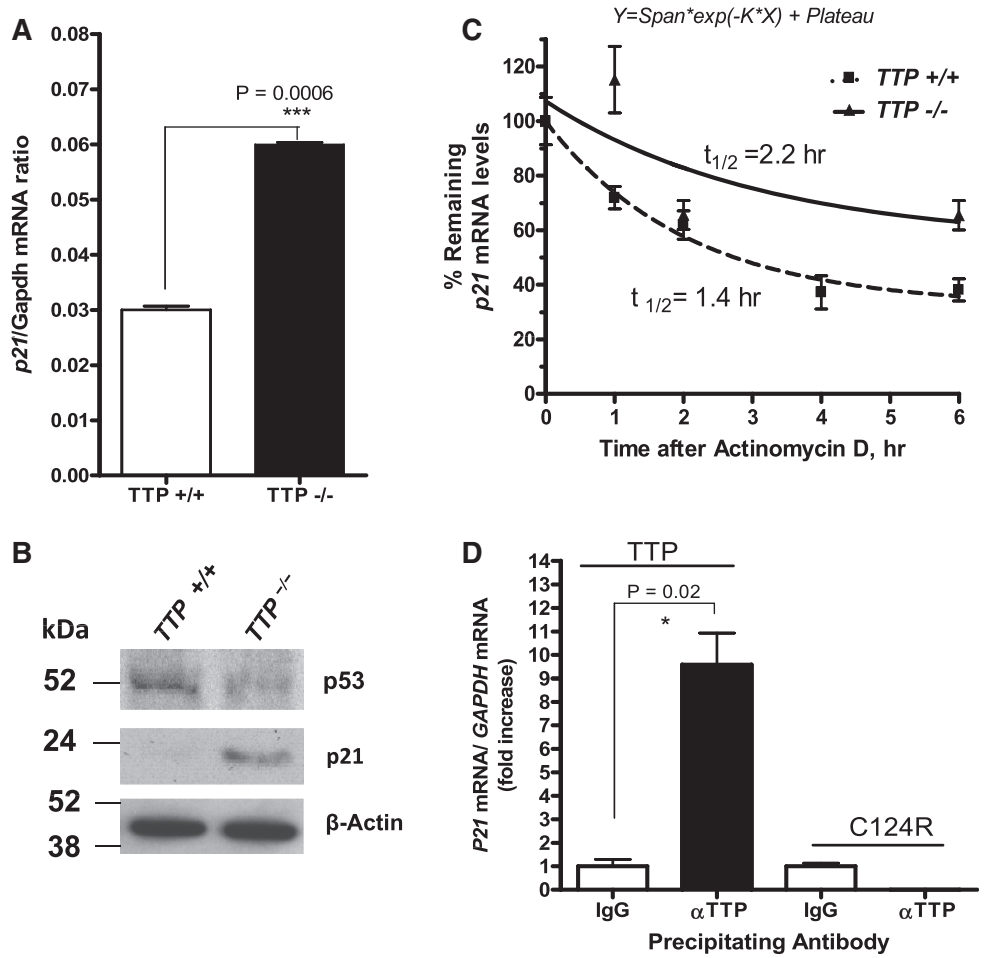

Figure 5. TTP regulates *p21* mRNA stability. (**A**) $TTP^{+/+}$ and $TTP^{-/-}$ MEFs were used to measure the expression of endogenous p21 transcript using QPCR. The expression was normalized to the mouse Gapdh housekeeping gene. The results are represented as the mean ± SEM of two independent experiments. ***$P = 0.0006$ (Student's *t*-test). (**B**) Immunoblotting for p53 and p21, using $TTP^{+/+}$ and $TTP^{-/-}$ MEFs total cell lysate. (**C**) TTP regulation of the *p21* mRNA half-life in $TTP^{+/+}$ and $TTP^{-/-}$ MEFs cells. (**D**) Real-time PCR of endogenous *p21* mRNA physically associated with wild-type or mutant TTP (C124R) and precipitated with anti-TTP antibody (IP-RNA details are given in 'Materials and Methods' section). The results are represented as the mean ± SEM of two independent experiments. *$P = 0.02$ (Student's *t* test).

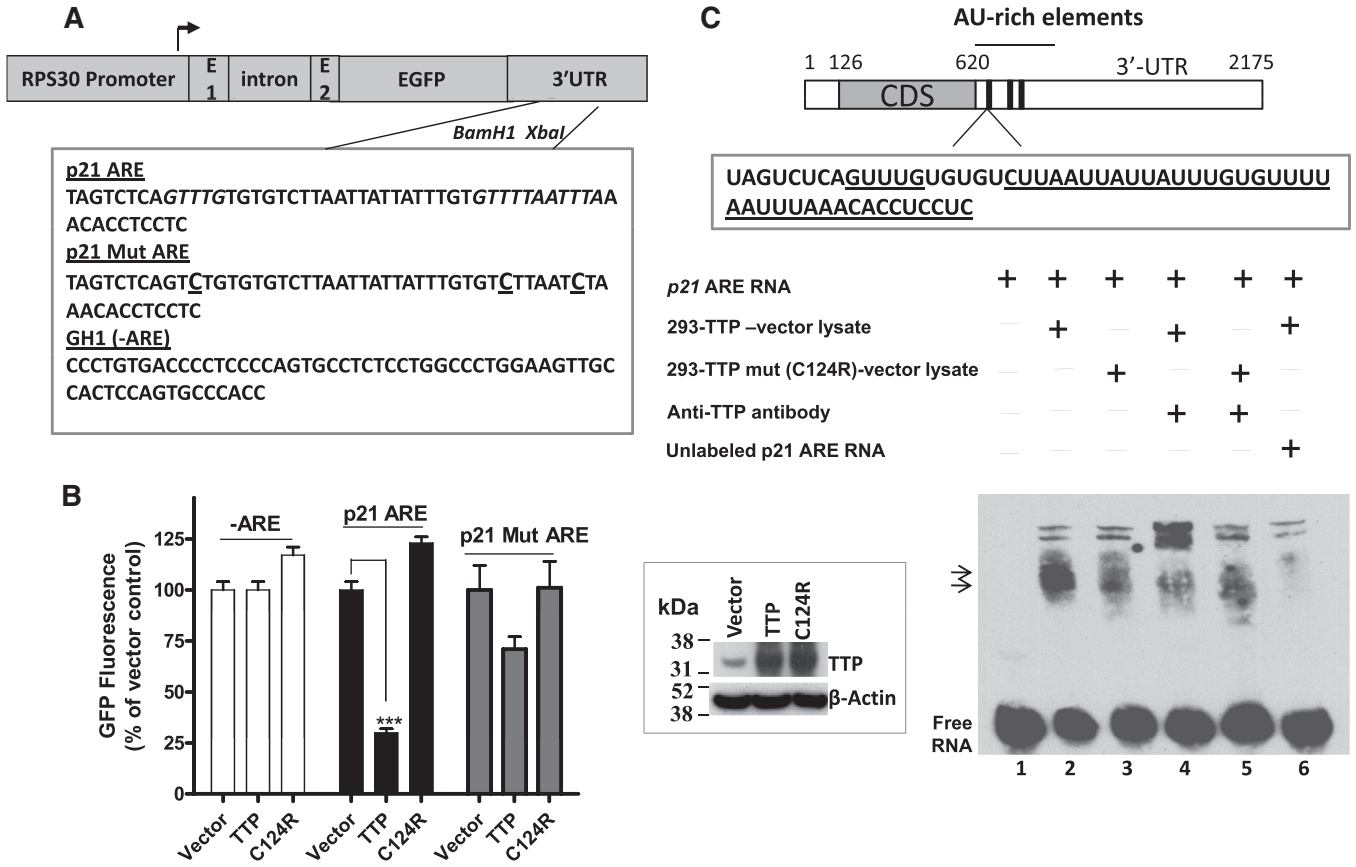

Figure 6. TTP regulation of p21 mRNA is AU-rich element-dependent. (**A**) Schematic diagram of control, p21 and p21 mutant ARE-containing EGFP reporter constructs under the control of the cellular promoter of ribosomal protein, RPS30 (20). (**B**) TTP regulation of p21 ARE-containing EGFP reporter activity. HEK293 cells were cotransfected with the indicated reporters along with control vector plasmid [PCR3.1, TTP, or C124R (mutant TTP)]. GFP fluorescence was measured 24 h post-transfection. The results are represented as the mean ± SEM of two independent experiments. ***$P < 0.001$ (Student's t test). (**C**) Upper panel, schematic diagram of p21 mRNA. The sequence of the p21 RNA probe used in RNA/EMSA is shown; ARE regions are underlined. Middle panel, electromobility gel shift assay (RNA-EMSA). The p21 ARE probe (lane 1) was incubated with 5 μg of TTP-overexpressing HEK293 (lanes 2) or C124R-overexpressing HEK293 cells (lane3) protein lysate. Arrows indicate the TTP-bound biotinylated RNA complex. A supershift assay was carried out in the same manner, except that protein lysate from TTP or C124R-overexpressing HEK293 protein lysates (lanes 4 and 5, respectively) were pre-incubated with anti-TTP antibody for 30 min before the addition of the biotinylated probe. The upper bands indicates the locations of supershifted band. A competition assay was carried out in the presence (+) of 1000-fold excess of unlabeled RNA competitor (lane 6). (Inset) A representative western blot for HEK293 cells overexpressing either wild-type TTP or mutant TTP (C124R) using anti-TTP or anti-β-actin antibodies.

of the C124R mutant caused no appreciable or statistically significant reduction in the reporter activity. As a control, mutant p21 ARE (p21 Mut ARE) of the same length (70 nt) was not able to trigger a significant reduction in the reporter activity (Figure 6B).

To further confirm that TTP can bind to the *p21* ARE region *in vitro*, an electromobility gel shift assay (EMSA) was performed using a biotinylated p21 ARE RNA probe. HEK293 cells were transfected with either wild-type TTP or mutant TTP (C124R) and subjected to the RNA-EMSA. One prominent ARE–protein complex (Figure 6C, lower panel, upper arrow) was observed to interact with p21 ARE in the lysate from cells expressing wild TTP but not with the mutant or unlabeled competitors (Figure 6C, lower panel lanes 2, 3 and 6, respectively). Both wild-type and mutant TTP expression were expressed to nearly the same amount (Figure 6D), but only mutant TTP was not able to bind the p21 ARE RNA. Moreover, the band from the lysates of the TTP vector-expressing cells is super-shifted with an anti-TTP antibody compared to the lysates from the TTP mutant vector-expressing cells, which did not super-shift the band (Figure 6C, lower panel lanes 4 and 5, respectively).

RNase L-mediated stabilization of p21 is TTP-dependent

To pinpoint the fact that RNase L induction of p21 occurs by the repression of TTP, we began a silencing experiment using TTP siRNA that led to >90% reduction of TTP protein (Figure 7A). We used Huh-7 cells (which express moderate levels of TTP in comparison to HEK293 cells, which do not) and transfected them with either RNase L expression vector or control vector. The p21 mRNA levels increased (2.8-fold, $P < 0.001$) due to TTP reduction by the specific siRNA (Figure 7B, Columns 1 and 3) which concur with the TTP knockout MEFs results (Figure 5A). In control siRNA treated cells, RNase L was able to

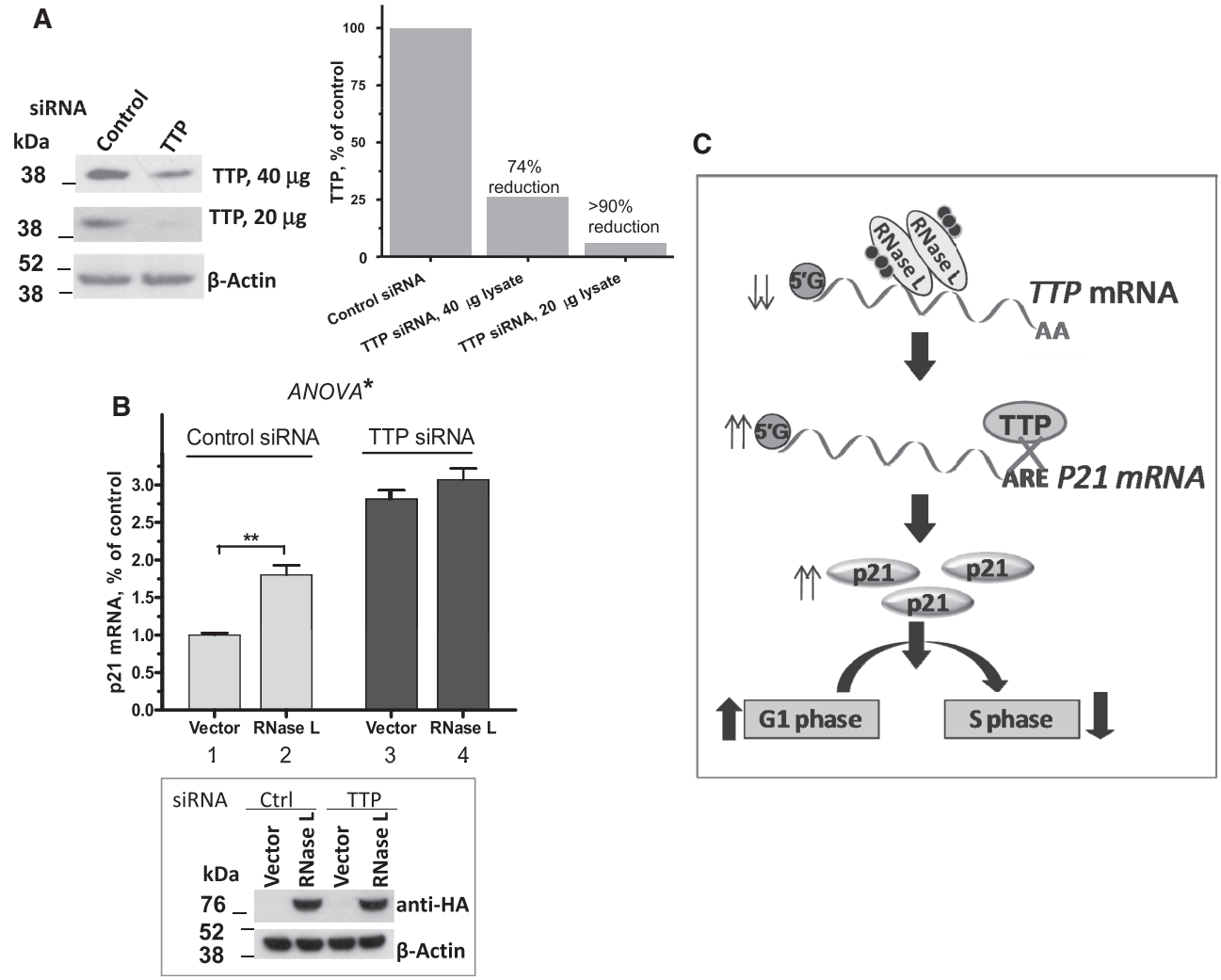

Figure 7. RNase L-mediated stabilization of p21 is enhanced by silencing TTP. (**A**) Huh-7 cells were transfected with TTP siRNA or control scrambled siRNA for 48 h. Two amounts of the lysates were used in western blotting for TTP using anti-TTP antibody (*left panel*) to assess knockdown efficiency (*right panel*). (**B**) Upper panel, real-time QPCR for p21 mRNA expression in TTP silenced cells. Huh-7 cells were transfected with TTP siRNA or control scrambled siRNA; 48 h later, the cells were transfected with vector control or RNase L plasmid. The results are represented as the mean ± SEM of two independent experiments. $^{**}P = 0.004$, (Student's *t*-test), * denotes $P < 0.01$, as assessed by ANOVA. Lower panel: western blotting for the transfected HA-RNase L. (**C**) The schematic diagram shows the proposed p21-mediated regulation of cell-cycle arrest by the RNase L-TTP axis. RNase L binds and degrades TTP mRNA resulting in lower level of TTP. TTP binds and degrades p21 mRNA in ARE-dependent manner, thus, the lower levels of TTP, lead to increased mRNA stability and subsequently increased p21 protein. The increased levels of p21 potentiate the G_1–S arrest of the cell cycle.

induce p21 mRNA as expected (Figure 7B, Columns 1 and 2). However, there was no increase in p21 mRNA levels due to RNase L when TTP levels were reduced by silencing with siRNA TTP (Figure 7A), indicating the requirement of TTP activity (Figure 7B, Columns 3 and 4). Taken together, these data demonstrate that the effect of RNase L on p21 mRNA is TTP-dependent.

DISCUSSION

Over the past decades, RNase L has been recognized as an endoribonuclease that degrades UU and UA di-ribonucleotides in viral mRNA as a part of the host defense against viruses (28). RNase L is also suggested as a tumor suppressor and is known to regulate apoptosis (1,4,8,29–33). Attention has been recently directed toward RNase L activity as a regulator of cellular mRNAs. Several reports by our group and others have supported the observation that RNase L modulates the stability of certain cellular mRNAs in the absence of viral infections, such as the RNA-binding protein ELAVL1 (HuR) (5), the double-strand RNA (dsRNA)-dependent protein kinase (PKR) (34), the muscle differentiation transcriptional factor (MyoD) (7), and the IFN stimulated genes 43 (ISG43) transcript (35). The putative effect of RNase L on cellular mRNA is not universal. The majority of cellular mRNAs and housekeeping mRNAs are not

affected (7,34–35). In the present study, we report that RNase L regulates an important pathway of cellular growth arrest, the $p21^{CIP1/WAF1}$ through a process that is dependent on an ARE-mediated event. This event is orchestrated by the ARE-binding protein, TTP, which we also find directly binds to p21 mRNA and promotes its decay.

RNase L is an important player in the IFN system. IFN has been used to treat certain types of human cancers, including HPV-associated cervical cancer, chronic myeloid leukemia and hepatic cancer (36–38). However, the exact IFN-mediated molecular mechanisms in cellular growth suppression remain largely elusive. IFN has been implicated in the upregulation of genes that inhibit cell growth and induce apoptosis. For instance, there was an identification of an IFN response element (ISRE) in the promoter region of p53 and subsequently of the IFN-mediated induction of p53 (39). Chelbi-Alix and colleagues showed that p53 is required for IFN-α induced apoptosis (40). Interestingly, IFN has been shown to target a specific component of the cell cycle. For example, IFN has been shown to upregulate the expression of p21, leading to G_1 arrest (41–45). Our results show that RNase L leads to G_1 arrest in a manner that was associated with p21 upregulation, as supported by both RNase L gain and loss experiments. Thus, the anti-proliferative activity of type-I IFNs (IFN-α and -β) involving the upregulation of p21 may be exerted through the OAS/RNase pathway. Earlier work showed that the overexpression of OAS, the upstream activator of the RNase L pathway, can inhibit cellular growth (46) and that overexpression of the dominant negative nuclease domain-deleted RNase L led to resistance to the anti-proliferative activity of IFN (47).

The present study provided different lines of evidence of the p21 upregulation by an RNase L-TTP axis. RNase L interacts physically with TTP mRNA, leading to a significant reduction in mRNA levels. This probably occurs via endoribonuclease activity because RNase L is known to cleave at the UU or UA dinucleotides (48) and the reduced levels were observed at the steady-state mRNA levels but the mRNA half-lives were not reduced. RNase L downregulation of TTP required both the dimerization and nuclease domain of the RNase L protein. The R462Q RNase L was originally described as a mutant form in hereditary prostate cancer and has a deficiency to dimerize to a catalytically active form; this variant has a significant reduction in the nuclease activity and reduced ability to mount apoptosis (33). Select cellular mRNAs can activate OAS, in the absence of viral infection, leading to the synthesis of 2–5A, the trigger of RNase L dimerization (49). Thus, basal levels of RNase L activity seems to be operative in intact cells due to certain cellular mRNA or small RNA fragments.

The requirement of the catalytic domain of RNase L (Figure 2E) was for both binding of RNase L to TTP mRNA and also for the nuclease activity confirming that the mRNA substrate binding is at C-terminus. Earlier (50) work showed that deletion of 10 amino acids (710–720) near the C terminus L of the 741 amino acid RNase L eliminated both the nuclease and RNA substrate-binding functions of the enzyme. Moreover, C-terminal truncated RNase L forms act as dominant negative inhibitor of the wild-type RNase L leading to attenuation of antiviral action of IFN (47); the dominant negative activity of RNase L mutants were also apparently seen in our experiments with p21 mRNA regulation.

The reduced TTP levels led to increases in both the level and half-life of p21. Unlike RNase L, which is an endoribonuclease, TTP is not a nuclease, but an mRNA-binding protein that binds ARE and subsequently recruits and activates mRNA decay enzymes that are involved in deadenylation and exonuclease activity (51,52). These activities require interactions with activation domains in the N- and C-terminus (52), while RNA binding occurs in the two zinc-finger domains in the middle of the TTP protein. The p21 mRNA contains AREs that recognize and bind to TTP, but not to the mutant TTP, which has a point mutation in one of the zinc-finger domains (Cys 124 to Arg 124). In a similar manner, several ARE-mRNAs are not recognized by the C124R mutant, as opposed to the wild-type protein, including TNF-α (27), Polo-Like Kinase 3 (53), ler3 (18), uPA(19), uPAR and MMP-1 (19). This is the first report that shows that p21 mRNA is a target for TTP. The p21 3′-UTR is long and contains multiple ARE sites that respond to different mRNA-binding proteins, including HuR, hnRNP K, RNPC1 and PCBP4 (14,54–57). In our study, the most functional ARE lies within the previously known HuR/HuD-binding region in the p21 3′-UTR (58).

The possible functional consequence of the RNase L-TTP axis in the regulation of p21 is cellular growth arrest (Figure 7C). RNase L was able to suppress cellular growth and cause growth arrest at the G_1/S phase, while the absence of RNase L caused accelerated growth and reduced growth arrest. RNase L activity can parallel the changes of OAS, the upstream activator of RNase L, during cell-cycle phases, wherein G_1/S arrest can be exerted by an optimal OAS/RNase L activity, (23) leading to p21 induction. This novel RNase L activity in regulating p21 occurs in an ARE-dependent manner that is orchestrated by TTP, a typical ARE binding and ARE-mRNA decay protein. G_1/S is an important regulatory step for p21 action, and this study offers a plausible explanation for the anti-proliferative mechanism of RNase L.

ACKNOWLEDGEMENTS

The authors thank Dr Wi S. Lai for the wild-type and knockout TTP MEF lines. The authors also thank Dr Robert H. Silverman (Lerner Research Institute, Cleveland, OH) for providing the RNase L mutant constructs and MEF lines. The authors are grateful to Dr Ghazi Alsbeih for his assistance with γ-radiation. The authors thank Mr Manogaran Pulicat for his technical assistance. The authors also acknowledge Mr. Maher Al-Saif for technical assistance.

FUNDING

The King Faisal Specialist Hospital and Research Centre (KFSH&RC) under the RAC proposal [# 2110 014]. Funding for open access charge: KFSH&RC.

Conflict of interest statement. None declared.

REFERENCES

1. Zhou,A., Paranjape,J., Brown,T.L., Nie,H., Naik,S., Dong,B., Chang,A., Trapp,B., Fairchild,R., Colmenares,C. *et al.* (1997) Interferon action and apoptosis are defective in mice devoid of 2′,5′-oligoadenylate-dependent RNase L. *EMBO J.*, **16**, 6355–6363.
2. Khabar,K.S., Dhalla,M., Siddiqui,Y., Zhou,A., Al-Ahdal,M.N., Der,S.D., Silverman,R.H. and Williams,B.R. (2000) Effect of deficiency of the double-stranded RNA-dependent protein kinase, PKR, on antiviral resistance in the presence or absence of ribonuclease L: HSV-1 replication is particularly sensitive to deficiency of the major IFN-mediated enzymes. *J. Interferon Cytokine Res.*, **20**, 653–659.
3. Bisbal,C. and Silverman,R.H. (2007) Diverse functions of RNase L and implications in pathology. *Biochimie*, **89**, 789–798.
4. Castelli,J.C., Hassel,B.A., Wood,K.A., Li,X.L., Amemiya,K., Dalakas,M.C., Torrence,P.F. and Youle,R.J. (1997) A study of the interferon antiviral mechanism: apoptosis activation by the 2-5A system. *J. Exp. Med.*, **186**, 967–972.
5. Al-Ahmadi,W., Al-Haj,L., Al-Mohanna,F.A., Silverman,R.H. and Khabar,K.S. (2009) RNase L downmodulation of the RNA-binding protein, HuR, and cellular growth. *Oncogene*, **28**, 1782–1791.
6. Zhou,A., Paranjape,J.M., Hassel,B.A., Nie,H., Shah,S., Galinski,B. and Silverman,R.H. (1998) Impact of RNase L overexpression on viral and cellular growth and death. *J. Interferon Cytokine Res.*, **18**, 953–961.
7. Bisbal,C., Silhol,M., Laubenthal,H., Kaluza,T., Carnac,G., Milligan,L., Le Roy,F. and Salehzada,T. (2000) The 2′-5′ oligoadenylate/RNase L/RNase L inhibitor pathway regulates both MyoD mRNA stability and muscle cell differentiation. *Mol. Cell. Biol.*, **20**, 4959–4969.
8. Andersen,J.B., Li,X.L., Judge,C.S., Zhou,A., Jha,B.K., Shelby,S., Zhou,L., Silverman,R.H. and Hassel,B.A. (2007) Role of 2-5A-dependent RNase-L in senescence and longevity. *Oncogene*, **26**, 3081–3088.
9. Nakayama,K. (1998) Cip/Kip cyclin-dependent kinase inhibitors: brakes of the cell cycle engine during development. *Bioessays*, **20**, 1020–1029.
10. Abbas,T. and Dutta,A. (2009) p21 in cancer: intricate networks and multiple activities. *Nat Rev Cancer*, **9**, 400–414.
11. Jung,Y.S., Qian,Y. and Chen,X. (2010) Examination of the expanding pathways for the regulation of p21 expression and activity. *Cell Signal*, **22**, 1003–1012.
12. Kuribayashi,K. and El-Deiry,W.S. (2008) Regulation of programmed cell death by the p53 pathway. *Adv. Exp. Med. Biol.*, **615**, 201–221.
13. Lafarga,V., Cuadrado,A., Lopez de Silanes,I., Bengoechea,R., Fernandez-Capetillo,O. and Nebreda,A.R. (2009) p38 Mitogen-activated protein kinase- and HuR-dependent stabilization of p21(Cip1) mRNA mediates the G(1)/S checkpoint. *Mol. Cell. Biol.*, **29**, 4341–4351.
14. Wang,W., Furneaux,H., Cheng,H., Caldwell,M.C., Hutter,D., Liu,Y., Holbrook,N. and Gorospe,M. (2000) HuR regulates p21 mRNA stabilization by UV light. *Mol. Cell Biol.*, **20**, 760–769.
15. Halees,A.S., El-Badrawi,R. and Khabar,K.S. (2008) ARED Organism: expansion of ARED reveals AU-rich element cluster variations between human and mouse. *Nucleic Acids Res.*, **36**, D137–D140.
16. Khabar,K.S. (2010) Post-transcriptional control during chronic inflammation and cancer: a focus on AU-rich elements. *Cell Mol. Life Sci.*, **67**, 2937–2955.
17. Stumpo,D.J., Lai,W.S. and Blackshear,P.J. (2010) Inflammation: cytokines and RNA-based regulation. *Wiley Interdiscip. Rev. RNA*, **1**, 60–80.
18. Lai,W.S., Parker,J.S., Grissom,S.F., Stumpo,D.J. and Blackshear,P.J. (2006) Novel mRNA targets for tristetraprolin (TTP) identified by global analysis of stabilized transcripts in TTP-deficient fibroblasts. *Mol. Cell. Biol.*, **26**, 9196–9208.
19. Al-Souhibani,N., Al-Ahmadi,W., Hesketh,J.E., Blackshear,P.J. and Khabar,K.S. (2010) The RNA-binding zinc-finger protein tristetraprolin regulates AU-rich mRNAs involved in breast cancer-related processes. *Oncogene*, **29**, 4205–4215.
20. Hitti,E., Al-Yahya,S., Al-Saif,M., Mohideen,P., Mahmoud,L., Polyak,S.J. and Khabar,K.S. (2010) A versatile ribosomal protein promoter-based reporter system for selective assessment of RNA stability and post-transcriptional control. *RNA*, **16**, 1245–1255.
21. Al-Zoghaibi,F., Ashour,T., Al-Ahmadi,W., Abulleef,H., Demirkaya,O. and Khabar,K.S. (2007) Bioinformatics and experimental derivation of an efficient hybrid 3′ untranslated region and use in expression active linear DNA with minimum poly(A) region. *Gene*, **391**, 130–139.
22. al-Haj,L., Al-Ahmadi,W., Al-Saif,M., Demirkaya,O. and Khabar,K.S. (2009) Cloning-free regulated monitoring of reporter and gene expression. *BMC Mol. Biol.*, **10**, 20.
23. Al-Ahmadi,W., Al-Ghamdi,M., Al-Haj,L., Al-Saif,M. and Khabar,K.S. (2009) Alternative polyadenylation variants of the RNA binding protein, HuR: abundance, role of AU-rich elements and auto-Regulation. *Nucleic Acids Res.*, **37**, 3612–3624.
24. Al-Ahmadi,W., Al-Ghamdi,M., Al-Haj,L., Al-Saif,M. and Khabar,K.S.A. (2009) Alternative polyadenylation variants of the RNA binding protein, HuR: abundance, role of AU-rich elements and auto-Regulation. *Nucleic Acids Res.*, **37**, 3612–3624.
25. Tchen,C.R., Brook,M., Saklatvala,J. and Clark,A.R. (2004) The stability of tristetraprolin mRNA is regulated by mitogen-activated protein kinase p38 and by tristetraprolin itself. *J. Biol. Chem.*, **279**, 32393–32400.
26. Brooks,S.A., Connolly,J.E. and Rigby,W.F.C. (2004) The role of mRNA turnover in the regulation of tristetraprolin expression: evidence for an extracellular signal-regulated kinase-specific, AU-rich element-dependent, autoregulatory pathway. *J. Immunol.*, **172**, 7263–7271.
27. Lai,W.S., Kennington,E.A. and Blackshear,P.J. (2002) Interactions of CCCH zinc finger proteins with mRNA: non-binding tristetraprolin mutants exert an inhibitory effect on degradation of AU-rich element-containing mRNAs. *J. Biol. Chem.*, **277**, 9606–9613.
28. Chakrabarti,A., Jha,B.K. and Silverman,R.H. (2011) New insights into the role of RNase L in innate immunity. *J. Interferon Cytokine Res.*, **31**, 49–57.
29. Carpten,J., Nupponen,N., Isaacs,S., Sood,R., Robbins,C., Xu,J., Faruque,M., Moses,T., Ewing,C., Gillanders,E. *et al.* (2002) Germline mutations in the ribonuclease L gene in families showing linkage with HPC1. *Nat. Genet.*, **30**, 181–184.
30. Castelli,J.C., Hassel,B.A., Maran,A., Paranjape,J., Hewitt,J.A., Li,X.L., Hsu,Y.T., Silverman,R.H. and Youle,R.J. (1998) The role of 2′-5′ oligoadenylate-activated ribonuclease L in apoptosis. *Cell Death Differ.*, **5**, 313–320.
31. Liu,W., Liang,S.L., Liu,H., Silverman,R. and Zhou,A. (2007) Tumour suppressor function of RNase L in a mouse model. *Eur. J. Cancer*, **43**, 202–209.
32. Urisman,A., Molinaro,R.J., Fischer,N., Plummer,S.J., Casey,G., Klein,E.A., Malathi,K., Magi-Galluzzi,C., Tubbs,R.R., Ganem,D. *et al.* (2006) Identification of a novel Gammaretrovirus in prostate tumors of patients homozygous for R462Q RNASEL variant. *PLoS Pathog.*, **2**, e25.
33. Xiang,Y., Wang,Z., Murakami,J., Plummer,S., Klein,E.A., Carpten,J.D., Trent,J.M., Isaacs,W.B., Casey,G. and Silverman,R.H. (2003) Effects of RNase L mutations associated with prostate cancer on apoptosis induced by 2′,5′-oligoadenylates. *Cancer Res.*, **63**, 6795–6801.
34. Khabar,K.S., Siddiqui,Y.M., al-Zoghaibi,F., al-Haj,L., Dhalla,M., Zhou,A., Dong,B., Whitmore,M., Paranjape,J., Al-Ahdal,M.N. *et al.* (2003) RNase L mediates transient control of the interferon response through modulation of the double-stranded

RNA-dependent protein kinase PKR. *J. Biol. Chem.*, **278**, 20124–20132.
35. Li,X.L., Blackford,J.A., Judge,C.S., Liu,M., Xiao,W., Kalvakolanu,D.V. and Hassel,B.A. (2000) RNase-L-dependent destabilization of interferon-induced mRNAs. A role for the 2-5A system in attenuation of the interferon response. *J. Biol. Chem.*, **275**, 8880–8888.
36. Koromilas,A.E., Li,S. and Matlashewski,G. (2001) Control of interferon signaling in human papillomavirus infection. *Cytokine Growth Factor Rev.*, **12**, 157–170.
37. Wadler,S. and Schwartz,E.L. (1990) Antineoplastic activity of the combination of interferon and cytotoxic agents against experimental and human malignancies: a review. *Cancer Res.*, **50**, 3473–3486.
38. Miyamoto,A., Umeshita,K., Sakon,M., Nagano,H., Eguchi,H., Kishimoto,S., Dono,K., Nakamori,S., Gotoh,M. and Monden,M. (2000) Advanced hepatocellular carcinoma with distant metastases, successfully treated by a combination therapy of alpha-interferon and oral tegafur/uracil. *J. Gastroenterol Hepatol.*, **15**, 1447–1451.
39. Takaoka,A., Hayakawa,S., Yanai,H., Stoiber,D., Negishi,H., Kikuchi,H., Sasaki,S., Imai,K., Shibue,T., Honda,K. *et al.* (2003) Integration of interferon-alpha/beta signalling to p53 responses in tumour suppression and antiviral defence. *Nature*, **424**, 516–523.
40. Chelbi-Alix,M.K., Quignon,F., Pelicano,L., Koken,M.H. and de The,H. (1998) Resistance to virus infection conferred by the interferon-induced promyelocytic leukemia protein. *J. Virol.*, **72**, 1043–1051.
41. Matsuoka,M., Tani,K. and Asano,S. (1998) Interferon-alpha-induced G1 phase arrest through up-regulated expression of CDK inhibitors, p19Ink4D and p21Cip1 in mouse macrophages. *Oncogene*, **16**, 2075–2086.
42. Sangfelt,O., Erickson,S., Castro,J., Heiden,T., Gustafsson,A., Einhorn,S. and Grander,D. (1999) Molecular mechanisms underlying interferon-alpha-induced G0/G1 arrest: CKI-mediated regulation of G1 Cdk-complexes and activation of pocket proteins. *Oncogene*, **18**, 2798–2810.
43. Sangfelt,O., Erickson,S., Einhorn,S. and Grander,D. (1997) Induction of Cip/Kip and Ink4 cyclin dependent kinase inhibitors by interferon-alpha in hematopoietic cell lines. *Oncogene*, **14**, 415–423.
44. Hobeika,A.C., Subramaniam,P.S. and Johnson,H.M. (1997) IFNalpha induces the expression of the cyclin-dependent kinase inhibitor p21 in human prostate cancer cells. *Oncogene*, **14**, 1165–1170.
45. Subramaniam,P.S. and Johnson,H.M. (1997) A role for the cyclin-dependent kinase inhibitor p21 in the G1 cell cycle arrest mediated by the type I interferons. *J. Interferon Cytokine Res.*, **17**, 11–15.
46. Rysiecki,G., Gewert,D.R. and Williams,B.R. (1989) Constitutive expression of a 2′,5′-oligoadenylate synthetase cDNA results in increased antiviral activity and growth suppression. *J. Interferon. Res.*, **9**, 649–657.
47. Hassel,B.A., Zhou,A., Sotomayor,C., Maran,A. and Silverman,R.H. (1993) A dominant negative mutant of 2-5A-dependent RNase suppresses antiproliferative and antiviral effects of interferon. *EMBO J.*, **12**, 3297–3304.
48. Wreschner,D.H., James,T.C., Silverman,R.H. and Kerr,I.M. (1981) Ribosomal RNA cleavage, nuclease activation and 2-5A(ppp(A2′p)nA) in interferon-treated cells. *Nucleic Acids Res.*, **9**, 1571–1581.
49. Molinaro,R.J., Jha,B.K., Malathi,K., Varambally,S., Chinnaiyan,A.M. and Silverman,R.H. (2006) Selection and cloning of poly(rC)-binding protein 2 and Raf kinase inhibitor protein RNA activators of 2′,5′-oligoadenylate synthetase from prostate cancer cells. *Nucleic Acids Res.*, **34**, 6684–6695.
50. Dong,B. and Silverman,R.H. (1997) A Bipartite Model of 2-5A-dependent RNase L. *J. Biol. Chem.*, **272**, 22236–22242.
51. Lai,W.S., Carballo,E., Strum,J.R., Kennington,E.A., Phillips,R.S. and Blackshear,P.J. (1999) Evidence that tristetraprolin binds to AU-rich elements and promotes the deadenylation and destabilization of tumor necrosis factor alpha mRNA. *Mol. Cell Biol.*, **19**, 4311–4323.
52. Lykke-Andersen,J. and Wagner,E. (2005) Recruitment and activation of mRNA decay enzymes by two ARE-mediated decay activation domains in the proteins TTP and BRF-1. *Genes Dev.*, **19**, 351–361.
53. Horner,T.J., Lai,W.S., Stumpo,D.J. and Blackshear,P.J. (2009) Stimulation of Polo-Like Kinase 3 mRNA Decay by Tristetraprolin. *Mol. Cell. Biol.*, **29**, 1999–2010.
54. Cho,S.J., Zhang,J. and Chen,X. (2010) RNPC1 modulates the RNA-binding activity of, and cooperates with, HuR to regulate p21 mRNA stability. *Nucleic Acids Res.*, **38**, 2256–2267.
55. Shu,L., Yan,W. and Chen,X. (2006) RNPC1, an RNA-binding protein and a target of the p53 family, is required for maintaining the stability of the basal and stress-induced p21 transcript. *Genes Dev.*, **20**, 2961–2972.
56. Yano,M., Okano,H.J. and Okano,H. (2005) Involvement of Hu and heterogeneous nuclear ribonucleoprotein K in neuronal differentiation through p21 mRNA post-transcriptional regulation. *J. Biol. Chem.*, **280**, 12690–12699.
57. Liu,J., Shen,X., Nguyen,V.A., Kunos,G. and Gao,B. (2000) Alpha(1) adrenergic agonist induction of p21(waf1/cip1) mRNA stability in transfected HepG2 cells correlates with the increased binding of an AU-rich element binding factor. *J. Biol. Chem.*, **275**, 11846–11851.
58. Joseph,B., Orlian,M. and Furneaux,H. (1998) p21waf1 mRNA contains a conserved element in its 3′-untranslated region that is bound by the Elav-like mRNA-stabilizing proteins. *J. Biol. Chem.*, **273**, 20511–20516.